In-flight deployment of morphing UAVs

A method to analyze dynamic stability, controllability and loads

Voskuijl, Mark; Muhammad Ridho Said, Muhammad Ridho; Pandher, Jaspreet; van Tooren, Michel; Richards, Blin

DOI
10.2514/6.2019-3126

Publication date
2019

Document Version
Final published version

Published in
AIAA Aviation 2019 Forum

AIAA AVIATION Forum
17-21 June 2019, Dallas, Texas
AIAA Aviation 2019 Forum

10.2514/6.2019-3126

In-flight deployment of morphing UAVs – a method to analyze dynamic stability, controllability and loads

Mark Voskuijl[1]
Netherlands Defence Academy, Faculty of Military Sciences, Den Helder, 1780AC, the Netherlands

Muhammad R. Said[2]
Delft University of Technology, Faculty of Aerospace Engineering, Delft, 2681HS, the Netherlands

Jaspreet Pandher[3]
Michel J. L. van Tooren[4]
University of South Carolina, College of Engineering and Computing, Columbia, South Carolina, 29208, United States

Blin Richards[5]
VX Aerospace, Morganton, North Carolina, 28655, United States

Several morphing unmanned aircraft systems which can be deployed in-flight are currently being developed for a variety of missions. Key to a successful in-flight deployment of these aircraft is that they enter a stable and controllable flight phase following a potentially highly dynamic transition phase without exceeding structural limitations. The aim of the current study is to develop a new physics-based methodology which can be used to assess under which flight conditions an unmanned morphing aircraft can be safely deployed in terms of stability, controllability and dynamic flight loads. The method is based on a Monte Carlo Simulation of the deployment phase with a multibody dynamics simulation model. As test case, the Dash X UAV is analyzed in combination with different deployment scenarios. Parameters to be varied are initial flight conditions such as body angular rates and the morphing strategy. The model is validated against a limited set of flight test data in its deployed state. Example results of the aircraft motion and loads are presented for safe deployments with a highly dynamic transition phase. The procedure to construct stability limits and deployment load envelopes is presented. The deployment load envelopes are a natural extension to the V-n diagram typically used for structural design. The stability limits can be used to determine the operational limits under which a UAV can be deployed safely without the risk of entering an unstable or uncontrollable flight regime. Ultimately, this method can be used to support the design of in-flight deployable morphing UAVs and the related operational procedures. It is demonstrated that the Dash X UAV can be safely deployed under realistic conditions with acceptable structural loads.

I. Nomenclature

h	=	Pressure altitude [m]	q	=	Pitch rate in aircraft body axes [deg/s]
H	=	Morphing actuator hinge moment [Nm]	r	=	Yaw rate in aircraft body axes [deg/s]
$\vec{L}$	=	Vector of flight load parameters	u	=	Longitudinal velocity, body axes [m/s]
M	=	Wing root bending moment [Nm]	v	=	Lateral velocity, body axes [m/s]
n	=	Load factor [-]	V_{ne}	=	Never exceed speed [m/s]
p	=	Roll rate in aircraft body axes [deg/s]	w	=	Vertical velocity, body axes [m/s]

[1] Professor, Military Sciences and Technology, AIAA member.
[2] Graduate Student, Aerodynamics, Wind Energy and Flight Performance and Propulsion.
[3] PhD Student, Smartstate™ Center for Multifunctional Materials and Structures. AIAA student member.
[4] Professor and Director Smartstate™ Center for Multifunctional Materials and Structures. AIAA member.
[5] Project Engineer, VX Aerospace Corporation.

$\vec{x}$	=	Vector of flight states
α	=	Angle of attack [deg]
γ	=	Flight path angle [deg]
ϕ	=	Roll attitude [deg]
θ	=	Pitch attitude [deg]
ψ	=	Yaw attitude [deg]
ARES	=	Aerial Regional-scale Environmental Survey
CFD	=	Computational Fluid Dynamics
DARPA	=	Defense Advanced Research Projects Agency
DATCOM	=	Data Compendium (US Air Force)
UAS	=	Unmanned Aircraft Systems
UAV	=	Unmanned Aerial Vehicle
UCAV	=	Unmanned Combat Aerial Vehicle
VLM	=	Vortex Lattice Method

II. Introduction

Over the last years, several research efforts have been initiated to develop small military drones which can be deployed in-flight by another aircraft. Northrop Grumman is investigating the use of a small drone called Dash X which fits inside a canister and can be dropped from a fighter aircraft [1, 2]. Once released, it deploys itself from the canister and unfolds its wings (Figure 1). The drone is primarily intended for reconnaissance. However, it could also be used for other combat and non-combat missions. The Defense Advanced Research Projects Agency (DARPA) is currently working on a project called Gremlins [3-5]. This project aims to develop Unmanned Aircraft Systems (UAS) which can not only be launched in-flight by a transport aircraft, bomber aircraft or fighter aircraft, but which can also be recovered in mid-air by a C-130 transport aircraft (Figure 2). Due to their size, small drones inherently have a low airspeed and limited range. This is a direct consequence of the well-known square cube law (relationship between volume and surface area as a shape increases or decreases in size, explained further in [6]). The main advantage of in-flight deployment is that small drones can be used at large distances from an airbase or aircraft carrier. With a small airframe they are more difficult to detect. In addition, the operational costs of small drones are relatively low. Their use also reduces risks for human operators in the field. Another military application is the use of a foldable glider which can be used as an air drop system (Figure 3). This idea is investigated by a technology demonstration project funded by DARPA. Recently, a successful flight test demonstration took place [7]. The foldable glider design can reach airspeeds up to 130 [kts] and glide over distances of 70 nautical miles. Rotorcraft and transport aircraft are potential platforms to deploy this aircraft from. It should be noted that the air launch of an unmanned aircraft is not new. Back in the 1950s, target drones were already launched in-flight. An example of two BQM-34S Firebee target drones mounted under the wing of a Lockheed DC-130 aircraft is provided in Figure 4 [8].

The possibility to store an unmanned aircraft and to deploy it in-flight is not limited to military applications. It can be highly advantageous in volume limited applications like space exploration where every cubic centimeter is important. In the field of space exploration, a concept for a Mars exploration aircraft was proposed to bridge the gap between the low-resolution but wide coverage data from Mars satellites and high resolution but narrow coverage data of the Mars rovers [9]. This is the idea behind the Mars Aerial Regional-scale Environmental Survey (ARES) aircraft and the concept was to transport a capsule containing the folded aircraft to the Martian atmosphere, reduce the speed of the capsule inside the Martian atmosphere by means of a parachute, and release the aircraft mid-air so that the aircraft can unfold itself and directly operate (Figure 5) [9]. More recently, Tao and Hansman [10] developed a micro-UAV which can be stored in a box and deployed in-flight at altitudes up to 35,000 ft. and Mach 0.8. In free fall, the box decelerates and at an airspeed of approximately 40 m/s, the micro-UAV is released and it unfolds itself (Figure 6). This system was successfully tested with a deployment from a helium balloon.

Key to a successful in-flight deployment of an unmanned aircraft is that it enters a stable and controllable flight phase following a potentially a highly dynamic transition phase. Furthermore, flight loads encountered during the dynamic transition phase should be within the structural flight envelope limits. Simulation of the flight dynamics and loads of vehicles which undergo large transformations by means of morphing is typically done using multibody-dynamics simulations in combination with a variety of aerodynamic methods. An et al. [11] successfully simulated the flight dynamics as a result of variable wing sweep. They developed a method to calculate the unsteady aerodynamic loads based on potential flow theory. Shi et al. [12] investigated the flight dynamics of large scale morphing aircraft based on a modified 6 DOF simulation approach. DATCOM [13] was used in their study to compute the aerodynamic loads. This method is however limited to low morphing rates. A multibody dynamics simulation model of an asymmetric aircraft with variable sweep was developed by Tong and Ji [14] with the aim to achieve roll control by changing the sweep angle. Details on the aerodynamic modelling method are not provided in their study. A mathematical approach to describe the dynamics of variable sweep aircraft with differential equations that employ time varying coefficients is provided by Bulekov and Teryev [15]. A tandem wing UAV with variable sweep was investigated by Gao et al. [16]. The multi-body dynamics was modelled using the Kane method [17]. For the

aerodynamics, both a vortex lattice method (VLM) and computational fluid dynamics (CFD, ANSYS Fluent) were used. Their main objective was to achieve flight control with variable wing sweep. Otsuka and Matahari [18] created a simulation model of the Mars explorer using flexible multibody dynamics with the aim to predict flutter of the wing. The effect of the rotation hinge of the wing on the aeroelasticity was included in their study. A configuration with folding wing was investigated by Yue et al. [19] by means of flexible multibody dynamics in combination with CFD. High wing fold angular velocities were simulated using a quasi-steady approach for the aerodynamic loads. The purpose of the study was to develop control algorithms for the transition phase. In [20] and [21], a new simulation tool is presented which can be used to simulate the loads on a morphing aircraft. The method is based on flexible multibody dynamics in combination with VLM. The loads on a folding wing UCAV were successfully simulated.

Fig. 1 Dash X UAV in folded configuration [2].

Fig. 2 Airborne recovery of Gremlin (adapted from [5]).

Fig. 3 Deployment flight test of foldable glider [7].

Fig. 4 Firebee target drones mounted under wing of Lockheed DC-130 [8].

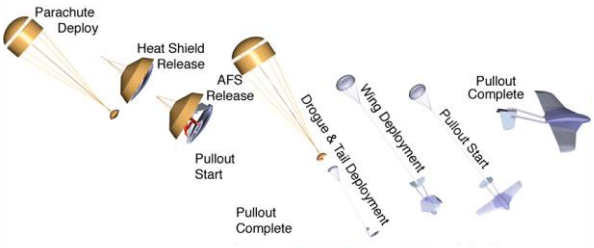

Fig. 5 Deployment procedure of Mars ARES aircraft (adapted from [9]).

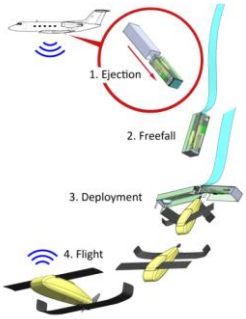

Fig. 6 Deployment procedure of micro-UAV [10].

The methods used by the research studies described above are mostly limited to relatively low morphing rates and low angular rates. In case a high morphing rate is simulated [22], the morphing motion is considered quasi-steady and the aircraft motion is limited to symmetric flight conditions. Furthermore, the aforementioned studies [11-21] do not deal with the exploration of the motion and loads in a highly dynamic deployment phase. Fujita et al. [22-24] on the other hand did explore the probability of a safe deployment for the ARES aircraft. A multibody dynamics approach was used to model the ARES aircraft. To represent the aerodynamics of the wings and tail surfaces, experimental aerodynamic data of flat plates for an angle of attack range of 360 degrees was used, at Reynolds numbers

representative for the Martian atmosphere. Aerodynamic interaction between different components of the aircraft were ignored. They used a '*sigma level*' method to evaluate the safety of deployment. Sigma stands for the standard deviation and a higher level indicates a lower dispersion. In this case, it indicates the probability of a safe deployment. This probability was quantified by determination of the sensitivity of the numerical simulation to variations in input parameters. Flight parameters varied were flight altitude, gust velocity and initial pitch angle. In addition, the method was used to investigate the effect of design parameters such as torque on the hinges of the wings on the deployment safety. Santoni and Gasbarri [25] also investigated the safety of deployment of a morphing aircraft in the Martian atmosphere. The different studies related to deployment in the Martian atmosphere are limited to longitudinal dynamics and a single deployment strategy (symmetric pull-up).

The aim of the current study is to develop a new physics-based methodology which can be used to assess under which flight conditions an unmanned morphing aircraft can be safely deployed in terms of stability, controllability and dynamic flight loads. It is applicable to any deployment strategy and includes lateral directional motion as well. The method is based on a Monte Carlo Simulation of the deployment phase in which initial flight conditions such as initial body angular rates, airspeed, altitude and turbulence levels are varied, as well as parameters that define the morphing strategy (wing deployment speed …). For each initial condition, the resulting nonlinear motion is characterized. In principle it can be stable, unstable or it can be a motion of a periodic nature (limit cycle). The result is essentially a safe deployment envelope, analogous to the well-known flight envelope. In addition, it gives a physical understanding of the motions beyond the safe deployment envelope. Besides the safety of the motion in terms of stability and controllability, the maximum and minimum loads encountered as a function of airspeed can also be quantified. The resulting deployment loads envelope is analogous to the maneuver and gust loads displayed in a conventional V-n diagram. The method can be used to assess all possible deployment strategies. To test the new physics-based methodology, the Dash X UAV configuration under development by Northrop and VX Aerospace is used as a test case. Three different deployment scenarios are investigated; (1) deployment from a canister which is slowed down by a parachute, (2) launch from under the wing of a fighter aircraft and (3) release from a cargo bay of a transport aircraft. The equations of motion of the unmanned aircraft are modelled using a multi (rigid) body dynamics simulation approach. For large sets of Monte Carlo Simulations, (unsteady) aerodynamic forces are represented by strip theory. Once a suitable deployment strategy is selected with a single morphing strategy, in combination with a limited range of initial flight conditions, high fidelity aerodynamic methods can be employed to accurately simulate the dynamics and loads.

This paper is structured as follows. First, an overview of the method to analyze an in-flight deployment is presented. This includes a description and validation of the multibody dynamics simulation model. Next, results for an example deployments under ideal conditions are presented. Following these basic simulations, deployment loads envelopes are presented for two scenarios based on an extensive set of simulations in which various initial conditions are varied. These deployment loads envelopes demonstrate the fitness of the new methodology for the problem at hand. Furthermore, the advantages and disadvantages of different deployment strategies will be explored based on the simulation results.

III. Deployment safety analysis methodology

The methodology to assess the safety of a deployment in terms of stability, controllability and flight loads is presented in this section. First the aircraft simulation model is described. Next, the different deployment strategies which will be investigated are described. These deployment strategies can be defined in terms of the range of initial flight conditions that can be expected and the procedures of morphing the aircraft system. Finally, the safety analysis method is detailed.

A. Aircraft simulation model

A multi-body dynamics simulation of the Dash X aircraft is created. The aircraft consists of six rigid bodies (fuselage, main wings, and horizontal and vertical tail surfaces). The rigid bodies are interconnected with force actuated revolute joints. The local angle of attack is measured along the span of the wings and tail surfaces. The aerodynamic force and moment acting on a wing section is calculated using quasi-steady two dimensional airfoil data which is stored within lookup tables as a function of Reynolds number, Mach number and local angle of attack. The dataset is based on wind tunnel data and covers the whole range of possible angles of attack (±180 degrees). The effectiveness of the control surfaces are estimated based on ESDU methods [26, 27]. In addition, limit control deflections are defined in the model. The overall simulation model is validated against flight test data for its deployed state. The responses of the aircraft as a result of a longitudinal, lateral and directional control inputs (doublet) are presented in Figures 7-9.

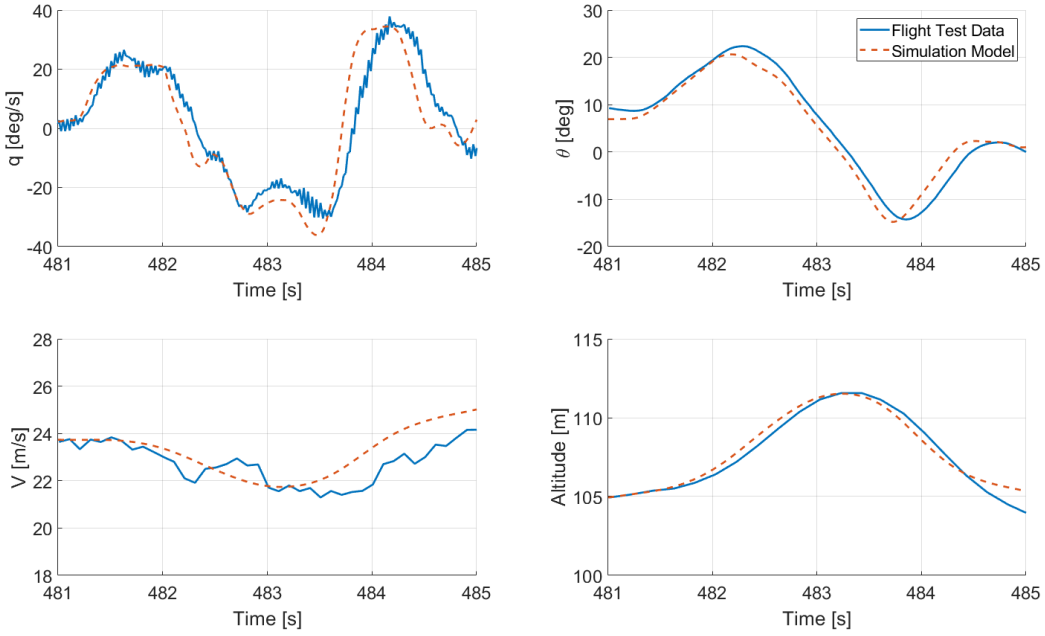

Fig. 7 Comparison of simulation model pitch response with flight test data for a pitch doublet.

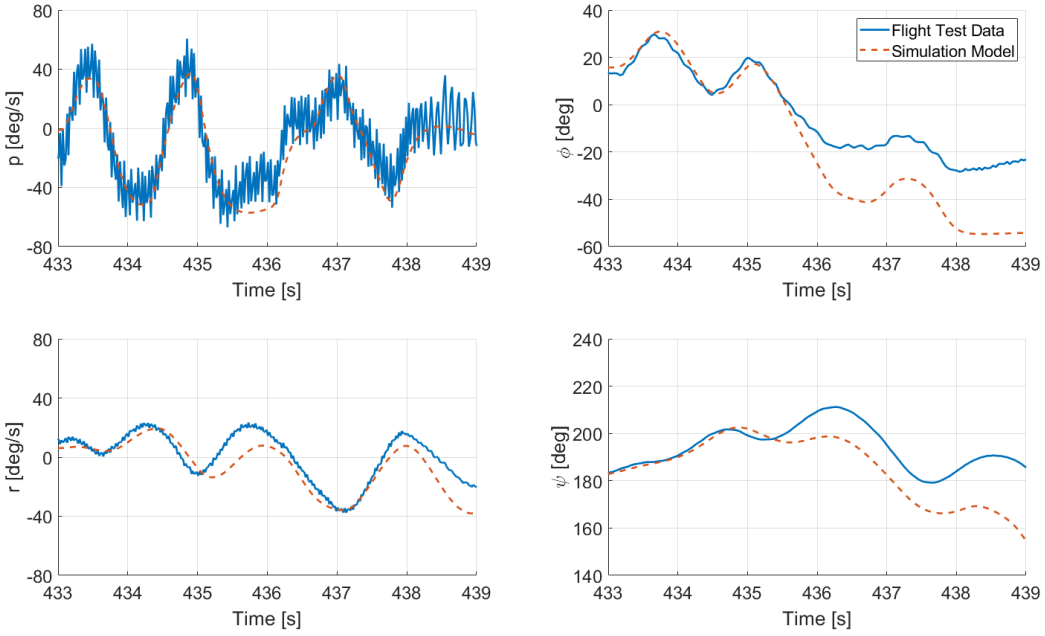

Fig. 8 Comparison of simulation model roll response with flight test data for a lateral doublet.

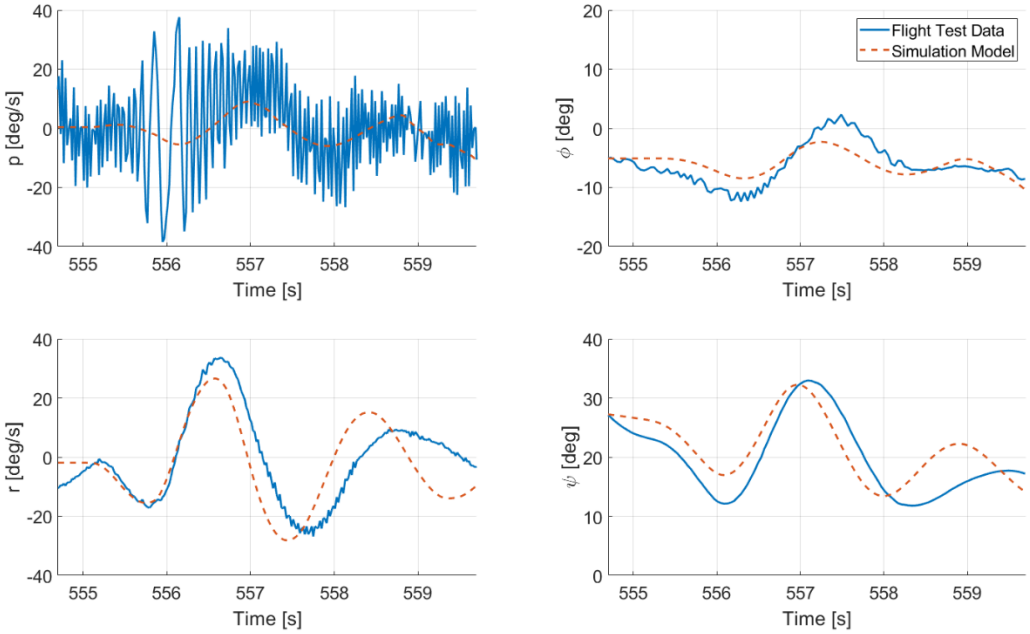

Fig. 9 Comparison of simulation model yaw response with flight test data for a directional doublet.

The measured control inputs from the flight test are used as input for the simulation model. Doublets are given in the three primary axes, however it should be noted at the same time small inputs are also given in the other axes. The measured control inputs in the flight test are used as input for the simulation. There are two inherent differences between the flight test maneuvers and the simulated maneuvers. First of all, the flight test data is not exactly trimmed at the start of the maneuvers. The accelerations are therefore small but nonzero and the angular rates do not necessarily match the angular rates corresponding to a steady flight condition. To trim the simulation model, a virtual pilot (control law) is used. This virtual pilot controls the airspeed, climb angle, roll angle and sideslip angle. Therefore, it can trim the simulation model in steady, uncoordinated climbing and descending turns. The accelerations of the simulation model are however zero after the trim process. As a consequence there is a discrepancy between the flight test data and the simulation at the very start of the comparison. These discrepancies gradually build up as time increases. Second, the exact wind condition in the flight test is unknown. For the comparison, there is no wind and turbulence in the simulation. Note that it is possible to trim a simulation model with accelerations present (unsteady flight) if a different type of trim algorithm is used. For the purpose of this validation, small discrepancies are deemed acceptable.

The comparison reveal that the pitch response of the simulation model matches the flight test data well. The lateral and directional responses show larger errors between the flight test and the simulation but still the simulation matches the flight test. This is most likely caused by the fact that the aircraft was less well trimmed during the flight test before the lateral and directional maneuvers were initiated. Other differences between the simulations and the flight test can be explained by the modelling approach. The influence of the main wing on the tail (downwash) is not modeled. The aerodynamics are modelled using quasi-steady two dimensional look-up tables and the structural components of the airframe are modelled perfectly rigid. In reality, the aircraft used in the flight test has some structural flexibility in the wing and the joints used for deploying the wing and tail surfaces.

Deployment strategies and initial flight conditions

A physics-based generic method to analyze the feasibility of an in-flight deployment should be suitable to any deployment strategy. Three different deployment scenarios are therefore considered in this study:

1) Deployment from a canister which is slowed down by a parachute.
2) Launch from under the wing of a fighter aircraft.
3) Release from a cargo bay of a transport aircraft.

The performance limits of the launch aircraft in terms of altitude and speed are different than the performance limits of the UAV since the launch aircraft has a larger weight. Therefore, the UAV has to transition from the deployment condition outside its own operational flight envelope to a flight condition within the operational flight envelope. This is schematically presented in Figure 10 for a launch from a representative supersonic fighter aircraft.

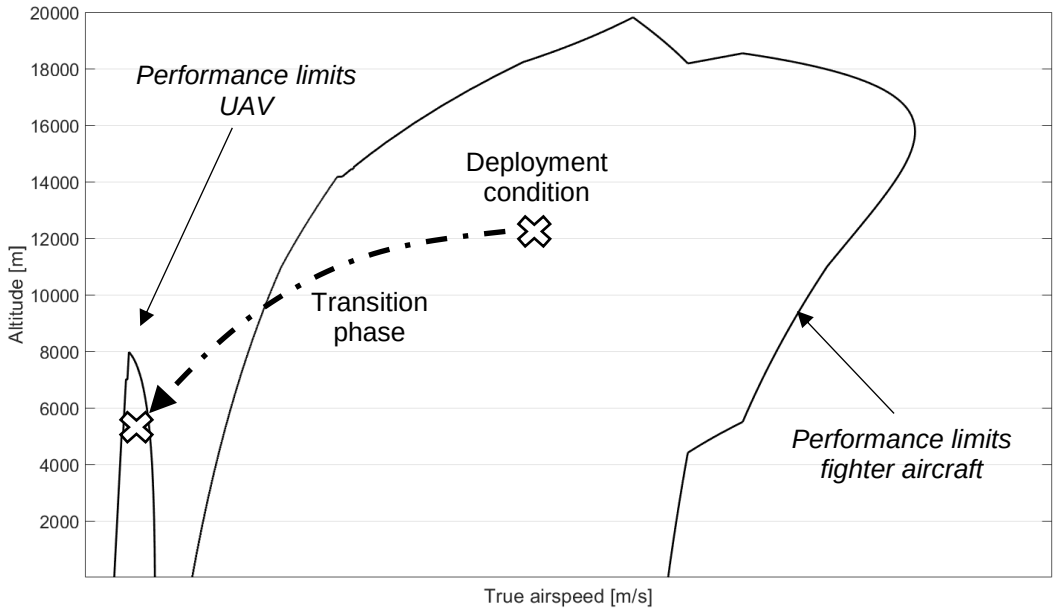

Fig. 10 Transition from deployment flight condition to an operational flight condition for scenarios 2 and 3

Following the release in free-air, the aircraft morphing procedure starts, which is visualized in Figure 11. The main steps are listed below.

1) Horizontal tail deployment – rotation about local yaw (vertical) axis.
2) Main wing (in-plane) rotation – rotation about local yaw (vertical) axis.
3) Main wing telescopic - extension along wing pitch (lateral) axis.
4) Vertical tail deployment – rotation about aircraft local pitch (lateral) axis.
5) Start of engine.

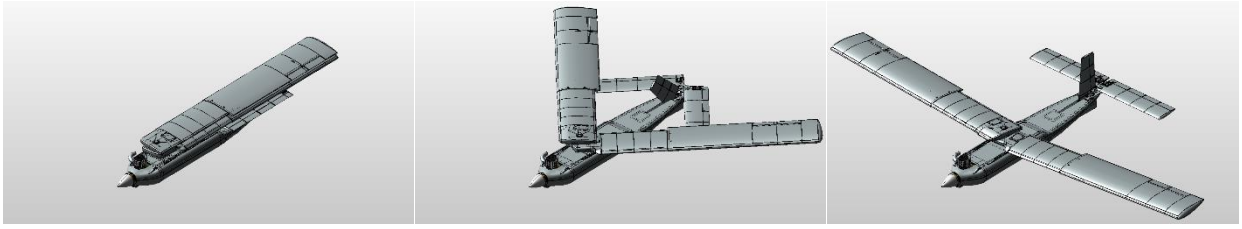

Fig. 11 Morphing sequence Dash X concept.

As initial condition for a simulation, the UAV is released from the aircraft or canister from an altitude (h) and in its folded shape. It may however have a nonzero initial translational velocity (u, v, w), angular velocity (p, q, r) and attitude (ϕ, θ, ψ) as a consequence of the dynamics of the release, atmospheric conditions and the flight state of the launch aircraft or canister, which may not be completely steady. The key difference between scenario 1 and the other two scenarios is the initial pitch attitude (nose down instead of horizontal) and the initial airspeed (close to zero compared to an airspeed equal to the true airspeed of the launch aircraft). During the transition phase in which the UAV morphs to its deployed flight state, the UAV will encounter flight loads. It is proposed to extend the traditional

V-n (airspeed - load factor) diagram with deployment loads as displayed in Figure 12. These loads will be encountered at airspeeds potentially beyond the design dive speed and typically at positive load factors.

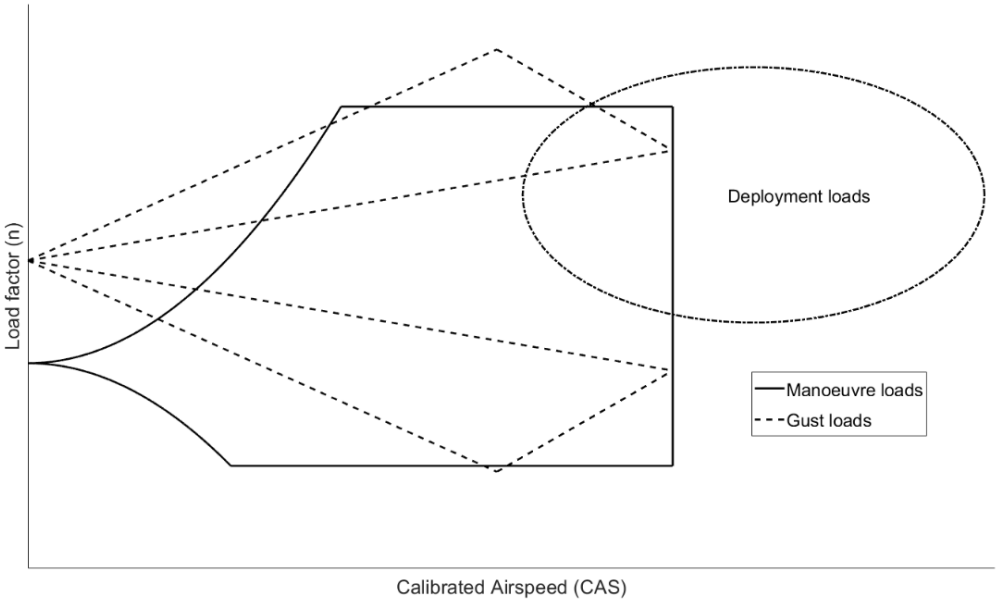

Fig. 12 Extension of the traditional V-n diagram with deployment loads.

It is essential that the dynamic motion of the aircraft results during the transition phase results in a stable flight condition. Whether or not the final motion is stable, unstable or of a periodic nature (limit cycle) depends on the initial flight state and atmospheric condition. This is schematically presented in Figure 13 for two initial flight condition deployment parameters. These parameters displayed on the axes can be initial translational velocities, angular rates, attitudes and atmospheric conditions. In reality, this will be a multidimensional picture since there are more than two parameters.

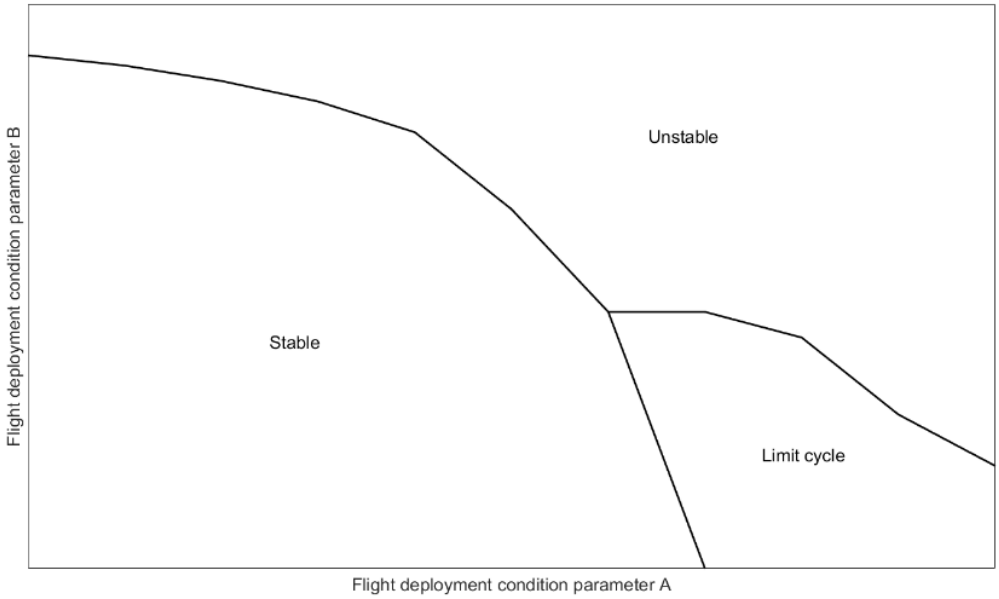

Fig. 13 Stability of motion as a function of the deployment flight condition.

B. Analysis method

To quantify the limits on the stability, controllability and flight loads following an in-flight deployment for a given scenario, it is proposed to make use of Monte-Carlo simulations. The initial conditions for a single simulation are the following.

$$\vec{x}_0 = [p \quad q \quad r \quad u \quad v \quad w \quad \phi \quad \theta \quad \psi \quad h] \tag{1}$$

The simulation model starts in its folded shape. The range of values considered for each flight state depends on the specific deployment scenario, the type of UAV to be launched and the atmospheric conditions. The current research is focused on developing a generic method that can be used for any scenario. Next, the trajectory of the UAV and the corresponding flight loads are analyzed for a given combination of initial states. For each simulation, the characteristic motion of the flight states is analyzed:

1) Stable (oscillatory or non-oscillatory).
2) Periodic motion (limit cycle).
3) Unstable (oscillatory or non-oscillatory).

The aim is to gain control of the UAV within a predefined timespan without exceeding structural limits. For each flight state, parameters related to flight loads which are considered are the following:

$$L = [n \quad V_{ne} \quad M_{wing} \quad M_{htail} \quad M_{vtail} \quad H_{htail} \quad H_{wing} \quad H_{vtail}] \tag{3}$$

Based on the available control power, the characteristic motion of the UAV and the dynamic loads, it is determined whether a deployment is successful or not for a specific simulation. Based on the results of all simulations, a "*safe deployment envelope*" is constructed. This is a set of diagrams, similar to a conventional flight envelope which displays under which combination of initial flight states a UAV can be launched successfully. As a final step, a limited number of safe trajectories which are most likely to be encountered in real-life, should be simulated with higher fidelity aerodynamic methods or validated with a controlled flight test. A schematic overview of all steps of the analysis method is presented in Figure 14.

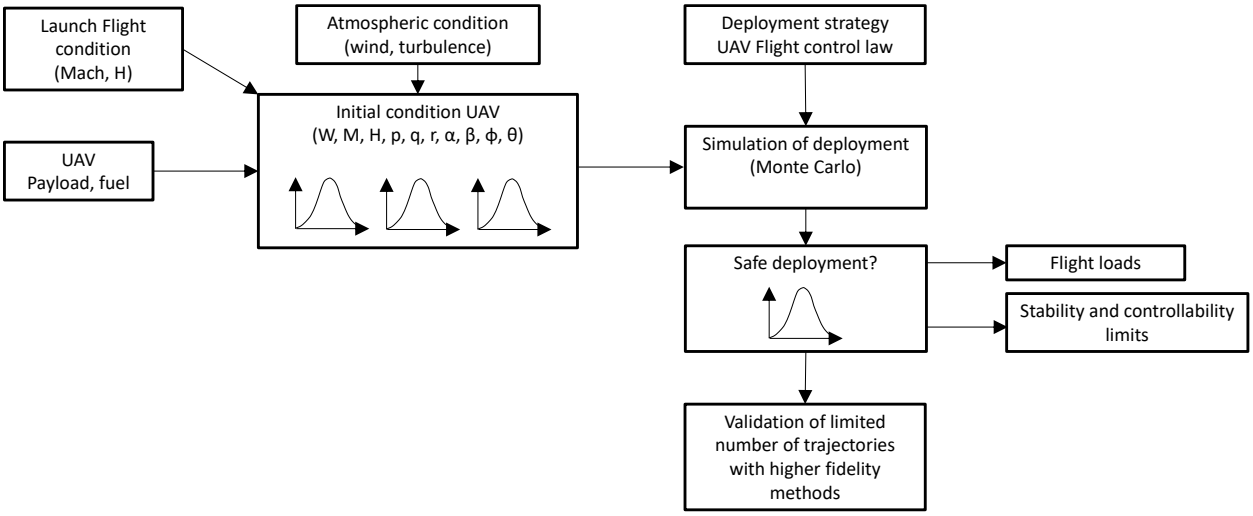

Fig. 14 Schematic overview analysis method.

IV. Results

Example results are presented in this section. First, a successful deployment from under the wing of an aircraft or from the cargo bay of a transport aircraft is presented in Figure 15. In this case, the initial condition is a pure horizontal steady and symmetric flight condition at 70 m/s and 4000 m altitude. This would be a rather low airspeed for a fighter

or transport aircraft and at the same time an airspeed higher than the maximum attainable airspeed in steady level flight for a small UAV.

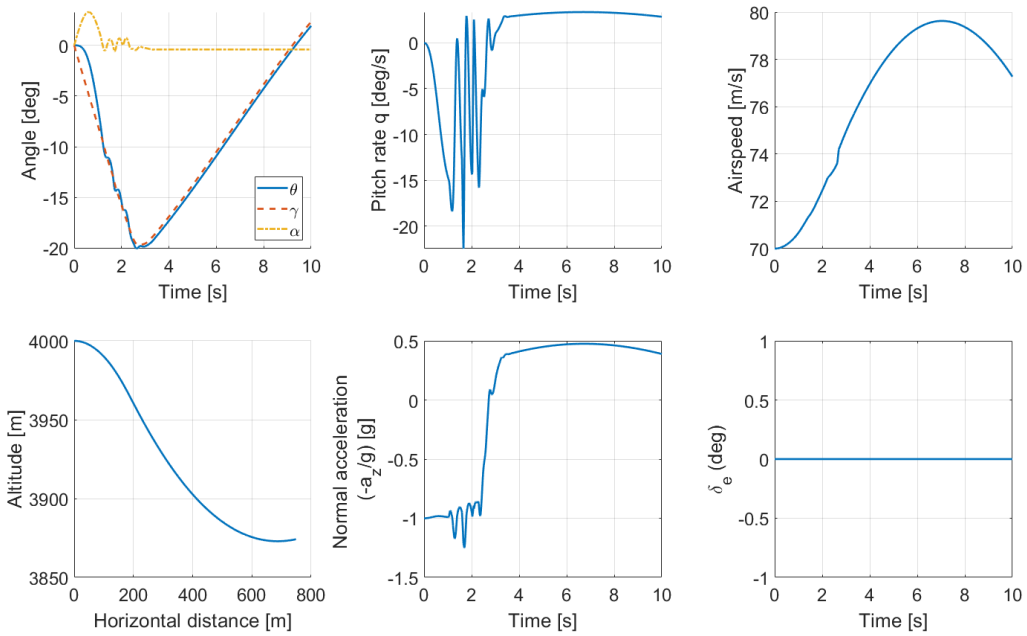

Fig. 15 Example successful in-flight deployment from under the wing or cargo bay of an aircraft.

It can be observed that directly after release, the UAV is in free-fall and the magnitude of the descent angle ($-\gamma$) increases due to an increasing rate of descent. At the same time, the angle of attack (α) increases. Next, several discrete events can be observed, particularly in the pitch rate response. First, the horizontal tail deploys, with no elevator deflection, which causes a nose down pitching moment and consequentially a negative pitch rate q and a decrease in the pitch attitude (θ). After the horizontal tail deployment, the main wing deploys in two steps. First there is a rotation about the yaw axis followed by a telescopic motion along the wing pitch axis present to increase the wing span. Finally, the vertical tail deploys. The mass of the vertical tail moves upwards and this can be seen as a small discrete event in the normal acceleration of the center of gravity. During the maneuver, the altitude drops and flight speed increases. The lateral and directional motion variables in this specific case remain quite small and they are therefore omitted from the figures. However, they are nonzero since the aircraft is not completely symmetric.

The successful deployment by means of a canister which is slowed down by a parachute is displayed in Figure 16. In this case, the UAV starts in a steady flight condition with a nose down attitude and a small vertical velocity of 5 m/s at an altitude of 2000 m. It can be seen that the UAV directly builds up speed at a descent angle of 90 degrees. The horizontal tail is deployed first with a constant negative elevator deflection of 10 degrees throughout the maneuver. This results in a nose-up pitch rotation. After the main wings are deployed, they start generating lift. This can be observed in a strong increase in the normal acceleration. Consequently, a pull-up maneuver is executed. When the UAV approaches a horizontal attitude, the airspeed levels off. Altogether, the UAV drops approximately 200 meter and at the same time an airspeed close to the maximum attainable level flight speed is obtained.

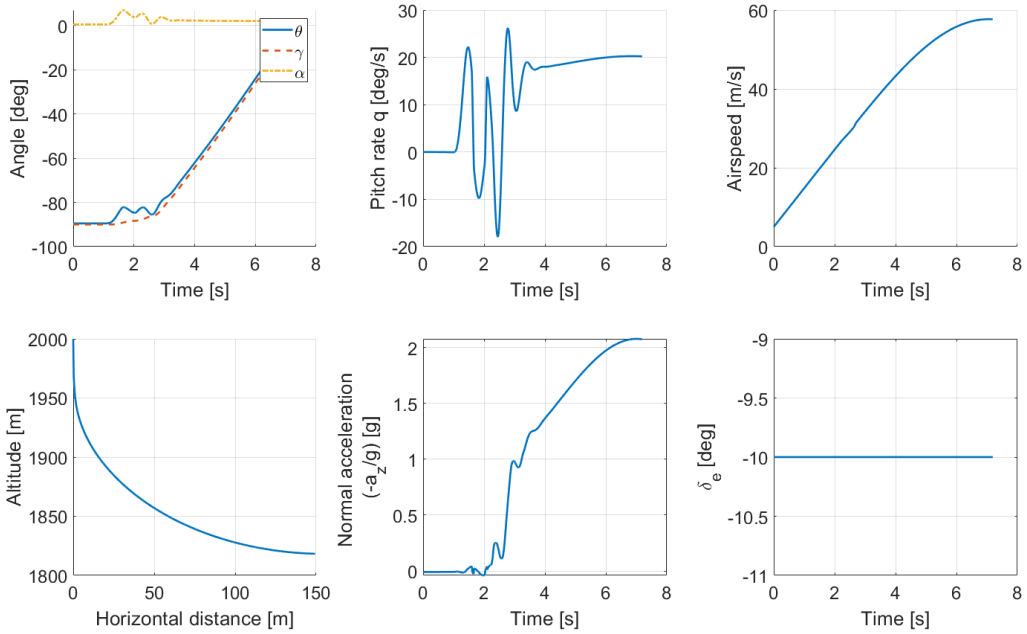

Fig. 16 Example successful in-flight deployment from canister.

The scenarios presented above are also analyzed for a range of initial flight conditions with different body angular rates and attitudes. These conditions are summarized in Table 1. Altogether, approximately 1000 simulations are performed per scenario in order to analyze the effect of all combinations of initial flight conditions. In all simulations, the aircraft controls are in a fixed position. For scenario 1, the aircraft has to perform a pull-up maneuver and therefore the elevator angle is set at a fixed negative position. Thus, there is no feedback control system active in any of the simulations. Clearly, an active control system can potentially increase the stability limits. The current simulations are focused on the analysis of the inherent stability without the interference of a control law.

	Scenario 1 Parachute / canister launch	Scenario 2/3 Wing mounted launch / Cargo bay launch
Roll rate [deg/s]	[-10, +10]	[-10, +10]
Pitch rate [deg/s]	[-10, +10]	[-10, +10]
Yaw rate [deg/s]	[-10, +10]	[-10, +10]
Forward velocity, u [m/s]	0	80
Lateral velocity, v [m/s]	0	0
Vertical velocity, w [m/s]	5	0
Bank angle [deg]	0	[-20, 20]
Pitch attitude [deg]	[-110, -70]	[-10, 10]
Altitude [m]	2000	4000
Elevator deflection [deg]	-10	0
Aileron deflection [deg]	0	0
Rudder deflection [deg]	0	0

Table 1. Initial flight conditions for all scenarios.

The resulting deployment load envelopes are presented in Figures 17 and 18. For each (calibrated) airspeed encountered during a simulation, the maximum and minimum accelerations are identified. The accelerations are measured in the center of gravity of the fully deployed UAV. They are defined in the aircraft body axes and divided by the gravitational acceleration. A convex hull (dashed lines) is drawn around these maximum and minimum accelerations to obtain the deployment load envelopes.

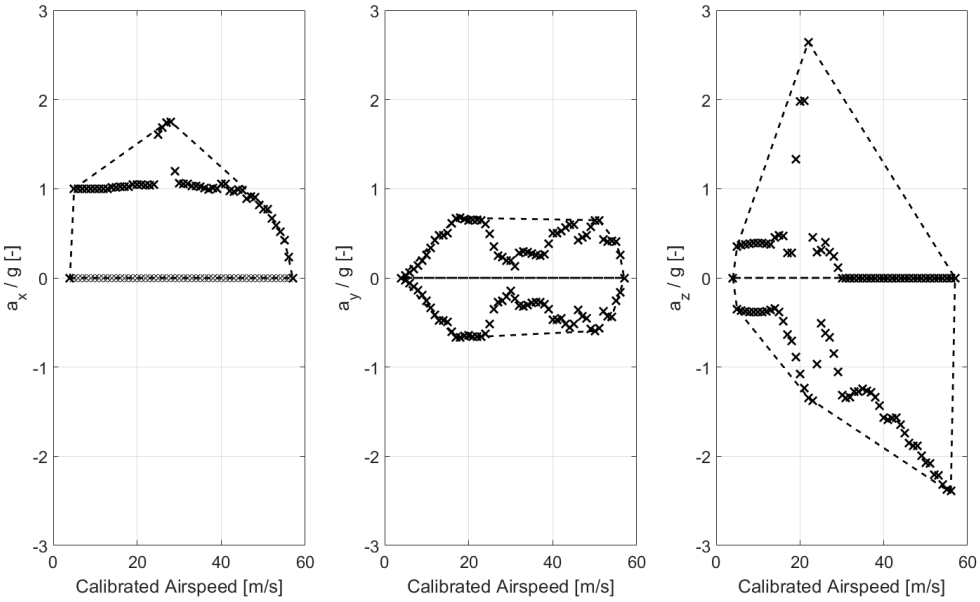

Fig. 17 Deployment load envelopes for release from a canister with a parachute.

For scenario 1 in which the UAV is deployed from a canister with a parachute, a peak normal acceleration load factor (a_z / g) of 2.5 'g' is encountered slightly above 20 m/s. At that speed, the main wings are deployed. Furthermore, the aircraft has a significant angle of attack at the moment of main wing deployment due to an initial pitch attitude smaller than -90 degrees and an initial positive pitch rate. Therefore, lift is created almost instantaneously when the main wings are deployed, inducing a pull-up maneuver. For structural design, these figures can be used in combination with the traditional V-n diagram based on gust loads and maneuver loads in normal deployed flight.

The same analysis was done for a wing mounted launch / cargo bay launch for a variety of initial conditions. The deployment load envelopes are presented in Figure 17. In this case, the lateral (a_y / g) and normal (a_z / g) acceleration load factors are larger. Especially the peak normal acceleration of almost 6 'g' at 65 m/s calibrated is notable.

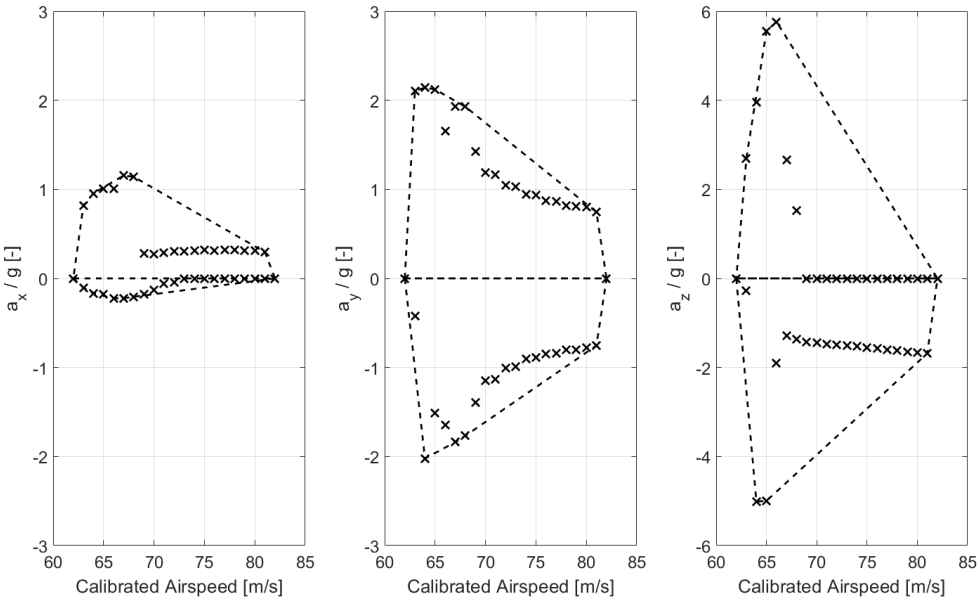

Fig. 18 Deployment load envelopes for wing mounted launch / cargo bay launch.

Finally, the stability after deployment is analyzed. This is done for scenarios 2 and 3. The stability after deployment for these scenarios is a function of 5 parameters (p, q, r, ϕ and θ). As an example, the stability of the motion after deployment is presented for a given initial pitch attitude (θ) of 3.3 [deg] and initial roll attitude (ϕ) of 20 [deg]. This flight condition could represent a steady level turning flight with a turn rate slightly lower than a rate one turn. The blue volume in Figure 19 represents the combinations of angular rates at the initial moment of deployment after which the morphing UAV achieves a stable flight condition. There is no control system active during the maneuver. At this specific flight condition, a large yaw rate, in combination with either a large pitch rate or roll rate results in an unstable motion. This example is merely intended as illustration. To have a full understanding of the stability limits, one would have to examine this figure for all flight conditions defined by initial pitch and roll attitude combinations.

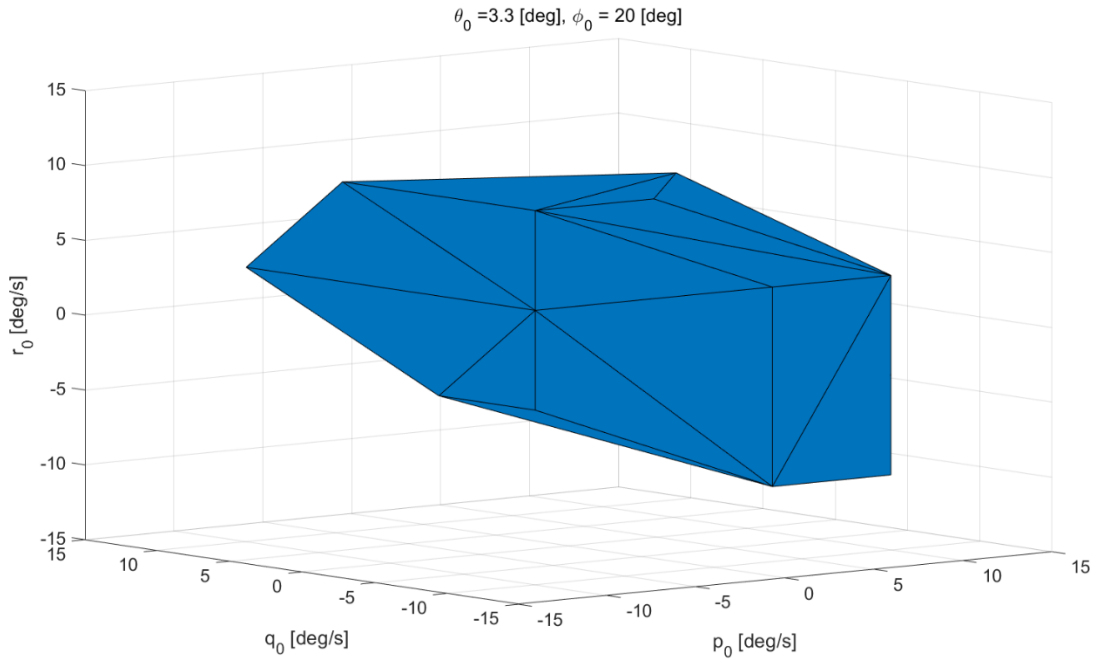

Fig. 19 Example stability limits for wing mounted launch / cargo bay launch.

Based on these calculated stability limits, it can be judged real-time in-flight whether a flight condition is safe for deployment in case the required parameters are measured.

V. Conclusions and recommendations

A new physics based method has been developed which can be used to assess the stability, controllability and flight loads of an in-flight deployment morphing UAV. The method relies on a multibody dynamics simulation model which can be used to simulate in-flight deployment of morphing aircraft. For a specific test case, the Dash X UAV configuration, this model is validated against a limited set of flight test data. Three in-flight deployment scenarios are analyzed for this test case. The procedure to construct stability limits and deployment load envelopes is presented. The deployment load envelopes are a natural extension to the V-n diagram typically used for structural design. The stability limits can be used to determine the operational limits under which a UAV can be deployed safely without the risk of entering an unstable or uncontrollable flight regime. Ultimately, this method can be used to support the design of in-flight deployable morphing UAVs and the related operational procedures.

In all deployment simulations, there are no atmospheric disturbances (turbulence / gusts). It is recommended to include gusts and turbulence in the Monte Carlo simulations. Since turbulence is a stochastic process, this is well suited for Monte Carlo simulations. Furthermore, the aerodynamic model can easily cope with a distributed, time-varying wind field. In order to increase the fidelity of the simulation model, it is recommended to extend the aerodynamic model with a semi-empirical dynamic stall model [28]. The morphing UAVs typically have several joints. It is a recommendation to analyze the effect of the flexibility of joints on the flight dynamics throughout the complete deployment maneuver and the operational flight envelope in the deployed state.

Acknowledgments

The authors would like to thank VX Aerospace for their help and assistance throughout the project.

References

[1] Tucker, P., "Northrop Tests Spy Drones That Deploy in a Fake Bomb," *Defense One*, Vol. 12, December 2017.
[2] Anonymous, [online picture] URL: http://vxaerospace.com/dash-x (Retrieved 29 October 2018)
[3] Wierzbanowski, S., "Gremlins," Defense Advanced Research Projects Agency, [online article] URL: https://www.darpa.mil/program/gremlins (retrieved 19 October 2018)
[4] Bosma, J., LTA 'aircraft carriers' of persistent, cheap microweaponized UAV swarms for fleet BMD overwatch, EW and wide-area ASW/surveillance," *23rd AIAA Lighter-Than-Air Systems Technology Conference, AIAA Aviation Forum,* Denver, Colorado, 2017.
[5] Anonymous, "Gremlins on track for demonstration flights in 2019," [online video] URL: https://www.darpa.mil/news-events/2018-05-09 (retrieved 19 October 2018)
[6] Torenbeek, E., "*Synthesis of Subsonic Airplane Design*," Delft University Press, The Netherlands, 1982.
[7] Sarigul-Klijn, M. M., Gionfriddo, M. P., Sarigul-Klijn, N., "Technology Demonstration of a 1-ton Single Use Disposable Glider," *AIAA SciTech Forum*, San Diego, California, 2019.
[8] Hambling, D., "A Short History of the Navy's Long Dislike of Drones," Popular mechanics, February, 2016. URL: https://www.popularmechanics.com/military/weapons/news/a19306/a-short-history-of-the-navys-long-dislike-of-drones/ (retrieved 2 May 2019).
[9] R. D. Braun, H. S. Wright, M. A. Croom, J. S. Levine, and D. A. Spencer, "Design of the ARES Mars Airplane and Mission Architecture," *Journal of Spacecraft and Rockets*, Vol. 43, No. 5, 2006, pp. 1026-1034.
[10] Tao, T.S., Hansman, R.J., "Development of an in-flight-deployable micro-UAV," *54th AIAA Aerospace Sciences Meeting*, San Diego, California, 2016.
[11] J. An, M. Yan, W. Zhou, J. X. Sun, Z. Yanf, and C. Qiu, "Aircraft Dynamic Response to Variable Wing Sweep Geometry," *Journal of Aircraft*, Vol. 25, No. 3, 1988, pp. 18-20.
[12] R. Shi and W. Wan, "Analysis of flight dynamics for large-scale morphing aircraft," *Aerospace Technology: An International Journal*, Vol. 87, No. 1, 2015, pp. 38-44.
[13] Williams, John E., Vukelich, Steven R. "*The USAF Stability and Control Digital DATCOM. Volume I. Users Manual*," Air Force Flight Dynamics Laboratory Technical Report AFFDL-TR-79-3032, Wright-Patterson Air Force Base, Ohio Nov. 1979.
[14] L. Tong, H. Ji, "Multi-body Dynamic Modelling and Roll Control of Asymmetric Variable Sweep Morphing Aircrafts," 2013 *10th IEEE International Conference on Control and Automation (ICCA)*, Hangzhou, China, 2013.
[15] V. P. Bulekov, E. D. Teryev, "Dynamics Variable Sweep Wing Aircraft In the Course of Changing Geometry," *IFAC 5th World Congress*, Proceedings Part 2, Paris, France, 1972, pp. 153-162.
[16] Gao, L., Jin, H., Zhao, J., Cai, H., Zhu, Y., "Flight Dynamics Modeling and Control of a Novel Catapult Launched Tandem-Wing Micro Aerial Vehicle With Variable Sweep," *IEEE Access*, Volume 6, 20 July 2018, pp. 42294-42308.
[17] Kane T R, and Levinson DA, "*Dynamics: theory and applications*", McGraw Hill, 1985.
[18] Otsuka, K., Makihara, K. "Aeroelastic deployable wing simulation considering rotation hinge joint based on flexible multibody dynamics," *Journal of Sound and Vibration*, Volume 369, 12 May 2016, pp. 147-167.
[19] Yue, T., Wang, L., Ai, J. "Multibody Dynamic Modeling and Simulation of a Tailless Folding Wing Morphing Aircraft," *AIAA Atmospheric Flight Mechanics Conference*, Chicago, Illinois, 2009.
[20] Reich, G.W. Bowman, J.C., Sanders, B., Frank, G.J. "Development of an integrated aeroelastic multibody morphing simulation tool," *47th AIAA/ASME/ASCE/AHS/ASC Structures, Structural Dynamics, and Materials Conference*, Newport, Rhode Island, 2006.
[21] Scarlett, J. N., Canfield, R. A., Sanders, B., "Multibody Dynamic Aeroelastic Simulation of a Folding Wing Aircraft," *47th AIAA/ASME/ASCE/AHS/ASC Structures, Structural Dynamics, and Materials Conference*, Newport, Rhode Island, 2006.
[22] K. Fujita, T. Motoda, and H. Nagai, "Numerical Analysis for an Aerial Deployment Motion of a Folded-Wing Airplane," *AIAA Atmospheric Flight Mechanics Conference - SciTech Forum and Exposition*, National Harbor, Maryland, 2014.
[23] K. Fujita, S. Kanagawa, and J. H. Nagai, "Robustness analysis on aerial deployment motion of a Mars aircraft using multibody dynamics simulation: effects of wing-unfolding torque and timing," *The Aeronautical Journal*, Vol. 121, No. 449, 2017, pp. 449–468.
[24] K. Fujita, T. Motoda, H. Nagai, "Dynamic Behaviour of Mars Airplane with Folded-Wing Deployment," *Transactions of the Japan Society for Aeronautical and Space Sciences*, Vol. 12, No. 29, 2014, pp. 1-6.
[25] Santoni, F., Gasbarri, P., "A deployable wing airplane supporting human landing on martian surface," *54th International Astronautical Congress of the International Astronautical Federation, the International Academy of Astronautics, and the International Institute of Space Law*, Bremen, Germany, 2003.
[26] ESDU Controls 01.01.03, "*Rate of change of lift coefficient with control deflection in incompressible two-dimensional flow, $(a_2)_0$*," ESDU International, with Amendments A and B, 1978.
[27] ESDU Wings 01.01.05, "*Slope of lift-curve for two-dimensional flow*," ESDU International, with Amendments A-E, 2007.
[28] McAlister, K. W., Lambert, O., Petot, D., "*Application of the ONERA model of dynamic stall*," NASA Technical Paper 2399, AVSCOM Technical Report 84-A-3, 1984.